Journal of Solid State Chemistry 184 (2011) 159–163

Contents lists available at ScienceDirect

Journal of Solid State Chemistry

journal homepage: www.elsevier.com/locate/jssc

# Syntheses, structures, thermal stabilities and luminescence of two new 3D zinc phosphonates

Ruibiao Fu *, Shengmin Hu, Xintao Wu *

*State Key Laboratory of Structural Chemistry, Fujian Institute of Research on the Structure of Matter, Chinese Academy of Science, Fuzhou, Fujian 350002, China*

ARTICLE INFO

*Article history:*
Received 16 July 2010
Received in revised form
15 October 2010
Accepted 8 November 2010
Available online 13 November 2010

*Keywords:*
Zinc
Phosphonate
Syntheses
Structure
Luminescence

ABSTRACT

A 1,4-Butanediamine has been introduced as a structure-directing agent to synthesize two 3D zinc phosphonates under hydrothermal conditions, $[(H_3N(CH_2)_4NH_3)\ Zn_2((O_3PCH_2)_2NCH_2PO_3H)(Cl)]$ (**1**) and $[(H_3N(CH_2)_4NH_3)Zn_3(O_3P(CH_2)_2PO_3)_2]$ (**2**). Compounds **1**∼**2** were characterized by single-crystal X-ray diffraction along with powder XRD, EA, IR and TGA. Compound **1** is a 3D open-framework consisting of tetranuclear units and 16-membered-ring channel. In compound **2**, each trinuclear unit contacts with surrounding six trinuclear units through O–P–O groups into a single hybrid layer, which is further pillared by $O_3P(CH_2)_2PO_3$ groups to form a 3D open-framework with 1D channel. In both compounds, 1,4-butanediamines are protonated and encapsulated into the channel through hydrogen bondings. Solids **1** and **2** are thermally stable up to 300 and 350 °C under air atmosphere, respectively. The luminescent properties of solids **1** and **2** are also studied in detail.



## 1. Introduction

Metal phosphonates have attracted extensive interest for their structural diversities and applications as porous materials, catalyst, ion-exchangers, Langmuir–Blodgett Film (LB), sensors and nonlinear optics [1]. During the last five years, metal phosphonates with fascinating structures and properties have continuously emerged as follows [2,3]. Phosphonic acids with additional functional groups like $NH_2$, OH, COOH, pyridyl, imidazole, triazole, thienyl and benzimidazol exhibit many coordination modes to form numerous solids, such as layered calcium tetraphosphonates undergoing a swelling upon $NH_3/H_2O$ uptake, $Co(2\text{-pmp})(H_2O)_2$ showing reversible changes of structures and magnetic behaviors upon the dehydration–hydration process, as well as porous heterometal phosphonate with helical channels and hydrogen sorption ability [4–13]. The combination of copper-bipyrimidine and molybdophosphonate clusters results in many hybrid materials [14]. Pillared metal diphosphonates have been exploited as meso/micro-porous materials [15–17]. Phosphonate clusters with manganese, iron, cobalt and copper, show interesting magnetism and strong third-order nonlinear optical (NLO) self-focusing effects [18–20]. Homochiral zinc and lanthanide phosphonates display 1D triple-strand helical chains and selective adsorption capacities for $N_2$, $H_2O$ and $CH_3OH$ molecules [21,22]. Furthermore, an important subject is to introduce organic amines as structure-directing agents to achieve various phosphonates, like mixed-valence vanadium phosphonoacetates with 16MR channels, and zinc phosphonates with tunable emission [23–28]. In this regard, Zheng et al. have successfully exploited 1,4-butanediamine as a structure-directing agent to tune the structures and properties of metal 1-hydroxyethylidenediphosphonates [29–35]. However, 1,4-butanediamine has not been introduced into metal nitrilotris (methylenephosphonates) and 1,2-ethylenediphosphonates. In this paper, we report syntheses, crystal structures, thermal stabilities and luminescence of two new 3D zinc phosphonates: $[(H_3N(CH_2)_4NH_3)Zn_2((O_3PCH_2)_2NCH_2PO_3H)(Cl)]$ (**1**) and $[(H_3N(CH_2)_4NH_3)Zn_3(O_3P(CH_2)_2PO_3)_2]$ (**2**).

## 2. Experimental

### 2.1. Materials and characterizations

$H_2O_3P(CH_2)_2PO_3H_2$ was prepared according to the previously reported method [36,37]. Other chemicals were obtained from commercial sources without further purification. Compounds **1**–**2** were synthesized in 25 mL Teflon-lined stainless steel vessels under autogenous pressure. The reactants were stirred homogeneously before heating. Elemental analyses were carried out with a Vario EL III element analyzer. Infrared spectra were obtained on a Nicolet Magna 750 FT-IR spectrometer. Photoluminescence properties for solids **1**–**2** were investigated under room temperature with FLS920 and LifeSpec-ps. While luminescent properties for 1,4-diaminobutane and acidified 1,4-diaminobutane solution were performed under room temperature with a F-7000 FL spectrophotometer. The diffuse reflectance spectra of solids **1**–**2** and 1,4-diaminobutane dihydrochloride were recorded on

* Corresponding authors. Fax: +86 591 83714946.
*E-mail address:* wxt@fjirsm.ac.cn (X. Wu).

0022-4596/$ - see front matter © 2010 Elsevier Inc. All rights reserved.
doi:10.1016/j.jssc.2010.11.013

a Perkin-Elmer Lambda 900 UV–vis-NIR spectrometer. Thermogravimetric analysis (TGA) was performed on a NETZSCH STA449C at a heating rate of 10 °C $min^{-1}$ from room temperature to 800 °C under air gas flow. Powder XRD patterns were acquired on a DMAX-2500 diffractometer using Cu$K\alpha$ radiation at an ambient environment.

### 2.2. Synthesis

$$[(H_3N(CH_2)_4NH_3)Zn_2((O_3PCH_2)_2NCH_2PO_3H)(Cl)] \quad (1)$$

A mixture of $Zn(CH_3COO)_2\cdot 2H_2O$ (0.3468 g, 1.580 mmol), $H_2N(CH_2)_4NH_2\cdot 2HCl$ (0.6346 g, 3.625 mmol), $(C_2H_5)_4NBr$ (1.5134 g, 7.201 mmol) and $H_6L$ solution (wt%=50%, 0.4 mL), with the pH value was adjusted to in the range 2–3, and then heated at 160 °C for 120 h. After slow cooling to room temperature, colorless prismatic crystals were obtained as a homogenous phase based on powder XRD patterns. Yield: 0.2576 g (59%). Anal. Calc. for $C_7H_{21}ClN_3O_9P_3Zn_2$: C 15.28, H 3.85, N 7.63%. Found: C 15.31, H 3.76, N 7.62%. IR (KBr pellet, $cm^{-1}$): 3099 m($\upsilon_{N-H}$), 2941w($\upsilon_{C-H}$), 2896w, 1631 m, 1509 m, 1468 w, 1436 m, 1236 m, 1227 m, 1174w($\upsilon_{P=O}$), 1113 s($\upsilon_{P-O}$), 1081 s($\upsilon_{P-O}$), 1051 s($\upsilon_{P-O}$), 999 m($\upsilon_{P-O}$), 981 m, 908 m, 775 m, 591 s and 576 m.

$$[(H_3N(CH_2)_4NH_3)Zn_3(O_3P(CH_2)_2PO_3)_2] \quad (2)$$

A mixture of $Zn(CH_3COO)_2\cdot 2H_2O$ (0.1149 g, 0.5235 mmol), $H_2N(CH_2)_4NH_2\cdot 2HCl$ (0.3507, 2.003 mmol), $(C_2H_5)_4NBr$ (1.2821 g, 6.100 mmol), $H_2O_3P(CH_2)_2PO_3H_2$ (0.1645 g, 0.8657 mmol) and $H_2O$ (8.0 mL, 444 mmol), with the pH value was adjusted to 5.4, and then heated at 180 °C for 144 h. After slow cooling to room temperature, colorless prismatic crystals were obtained as a homogenous phase based on powder XRD patterns. Yield: 0.0884 g (77%). Anal. Calc. for $C_8H_{22}N_2O_{12}P_4Zn_3$: C 14.60%, H 3.37%, N 4.26%. Found: C 14.45%, H 3.06%, N 4.25%. IR (KBr pellet, $cm^{-1}$): 3005 w($\upsilon_{N-H}$), 2931 m($\upsilon_{C-H}$), 2970 w, 2806 w, 2632 w, 2112 w, 1526 m, 1652 m, 1452 w, 1298 w, 1263 w, 1196 m($\upsilon_{P=O}$), 1124 s($\upsilon_{P-O}$), 1108 s($\upsilon_{P-O}$), 1071 s($\upsilon_{P-O}$), 1047 s($\upsilon_{P-O}$), 1013 s($\upsilon_{P-O}$), 986 s, 807 w, 758 m and 537 m.

### 2.3. X-ray crystallography

X-ray data for **1**–**2** were collected at 293(2) K on a Rigaku Mercury CCD/AFC diffractometer, using graphite-monochromated Mo-$K\alpha$ radiation ($\lambda$(Mo-$K\alpha$)=0.71073 Å). Data of **1**–**2** were reduced with CrystalClear v1.3. Their structures were solved by direct methods and refined by full-matrix least-squares techniques on $F^2$ using SHELXTL-97 [38]. All non-hydrogen atoms were treated anisotropically. Hydrogen atoms were generated geometrically. Crystallographic data for **1**–**2** are summarized in Table 1. CCDC 782688 (**1**) and 782689 (**2**).

**Table 1**
Crystallographic data for compounds **1** and **2**.

| Compound | **1** | **2** |
|---|---|---|
| Formula | $C_7H_{21}ClN_3O_9P_3Zn_2$ | $C_8H_{22}N_2O_{12}P_4Zn_3$ |
| FW | 550.37 | 658.27 |
| Space group | $P2(1)/n$ | $P-1$ |
| $a$ (Å) | 8.130(3) | 9.0800(17) |
| $b$ (Å) | 22.358(7) | 14.939(6) |
| $c$ (Å) | 10.538(3) | 28.994(12) |
| $\alpha$ (deg.) | 90 | 78.18(2) |
| $\beta$ (deg.) | 112.357(3) | 88.974(9) |
| $\gamma$ (deg.) | 90 | 89.72(2) |
| $V$ (Å$^3$) | 1771.5(10) | 3849(2) |
| $Z$ | 4 | 8 |
| $T$(K) | 293(2) | 293(2) |
| Measured/unique/ observed reflections | 13,523/4036/3545 | 28,866/17,104/7558 |
| $D_{calcd}$ (g cm$^3$) | 2.064 | 2.272 |
| $\mu$ ($mm^{-1}$) | 3.178 | 4.106 |
| GOF on $F^2$ | 1.076 | 1.039 |
| $R_{int}$ | 0.0419 | 0.0959 |
| $R1$[a] [$I>2\sigma(I)$] | 0.0556 | 0.1441 |
| w$R2$[b] [all data] | 0.1660 | 0.4351 |

[a] $R1=\sum(||F_o|-|F_c||)/\sum|F_o|$.
[b] $wR2=\{\sum w[(F_o^2-F_c^2)]/\sum w[(F_o^2)^2]\}^{0.5}$.

## 3. Results and discussion

### 3.1. Structural descriptions

The asymmetric unit of **1** includes two crystallographically independent Zn(II) ions, one $(O_3PCH_2)_2NCH_2PO_3H$ group, one $Cl^-$ anion and a protonated 1,4-butanediamine cation. As shown in Fig. 1, Zn1 ion is surrounded by two $(O_3PCH_2)_2NCH_2PO_3H$ groups into a distorted [$ZnO_4N$] trigonal bipyramidal coordination geometry. It is attractive that one $(O_3PCH_2)_2NCH_2PO_3H$ group is chelated to the Zn1 ion *via* three phosphonate oxygen atoms (O3, O5 and O8a) on the basal plane, along with a nitrogen donor (N1) occupying one polar site. To the best of our knowledge, the chelating mode is rare and only reported in [Hpy][Cu(N($CH_2$-$PO_3H$)$_3$)($H_2O$)], due to the nitrogen atom in other compounds is protonated [39–47]. And the other polar site of [$ZnO_4N$] trigonal bipyramid is occupied by the fourth phosphonate oxygen atom (O9) from another $(O_3PCH_2)_2NCH_2PO_3H$ group. While the Zn2 ion is in a distorted [$ZnO_3Cl$] tetrahedral coordination geometry defined by three oxygen atoms from three different $(O_3PCH_2)_2NCH_2PO_3H$ groups and one $Cl^-$ anion. The bond lengths of Zn–O lie in the range 1.915(4)~2.034(4) Å, which match with those of zinc phosphonates [27]. The bond lengths of Zn1–N1 and Zn2–Cl1 are 2.304(4) and 2.3021(13) Å, respectively, which are longer than those of zinc phosphonates [7,22,48–49]. On the other hand, the $(O_3PCH_2)_2$ $NCH_2PO_3H$ group exhibits a new octadentate mode to combine five Zn ions through seven phosphonate oxygen atoms along with one nitrogen donor. It is worth to mention that the nitrogen atom is not protonated and takes part in coordination. This is different from those in the reported compounds [40–47]. In addition, there are four hydrogen bondings in this structure: (1) the protonated 1,4-butanediamine provides three hydrogen atoms to form hydrogen bondings with adjacent phosphonate groups (N2···O5, 2.816(6) Å; N3···O3, 2.816(6) Å; N3···O8d, 2.892(7) Å); (2) the protonated phosphonate oxygen atom (O7) interacts with the neighboring phosphonate oxygen atom (O2e) through a strong hydrogen bonding (O7···O2e, 2.460(6) Å).

Thus, adjacent two Zn2 ions are bridged by two O4–P2–O6 into a binuclear unit. And the binuclear unit contacts with neighboring two Zn1 ions via O5 atoms to form a tetranuclear unit. On the *bc* plane, each tetranulcear unit contacts with surrounding four tetranulcear units through O9 to form a 2D hybrid layer. While along an *a* axis, adjacent tetranulcear units interact each other with O1 to form a chain. Thus, each tetranuclear unit contacts with surrounding six tetranuclear units to form a 3D framework with 16 MR channel along an *a* axis. The $Cl^-$ ion points to the channel. And the channel is occupied by the protonated 1,4-butanediamine cations, which interacts to the 3D framework with hydrogen bonding.

Suitable single-crystal XRD reveals that solid **2** crystallize in the central space group $P-1$ with 3D pillared framework (Fig. 2). All Zn ions are in [$ZnO_4$] distorted tetrahedral coordination geometries, which are surrounded by four oxygen atoms from four different $O_3P(CH_2)_2PO_3$ groups. The bond lengths of Zn–O are in the range 1.881(14)~2.043(4) Å, which match with those in **1**. On the other hand, each $O_3P(CH_2)_2PO_3$ group exhibits a hexadentate mode to combine six Zn ions through all deprotonated oxygen atoms, which

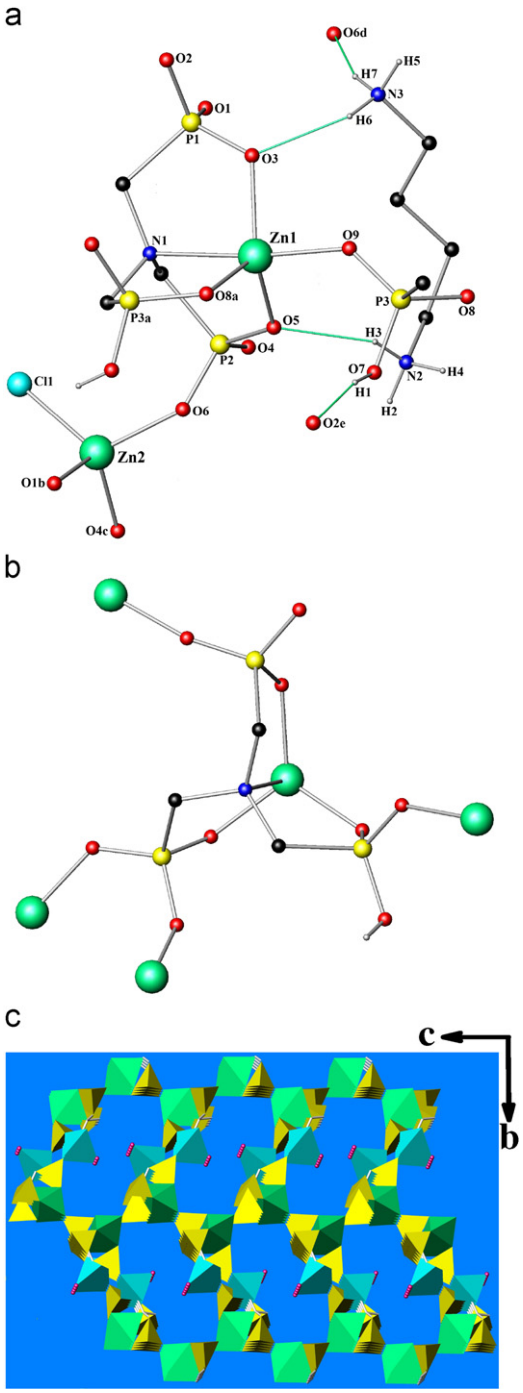


**Fig. 1.** Ball-stick view of (a) the coordinated environment of Zn ions, (b) the coordination mode of $(O_3PCH_2)_2NCH_2PO_3H$ group and (c) polyhedral view of the 3D framework in **1**. Blue-green lines represent hydrogen bonding. Unrelated hydrogen atoms are omitted for clarity. Symmetry codes: $ax-1/2,-y+1/2,z-1/2$; $bx-1,y,z$; $c-x-1,\ -y,-z+1$; $dx+1,\ y,\ z$; $ex-1/2,\ -y+1/2,\ z+1/2$. [$ZnO_4N$]: green trigonal bipyramid; [$ZnO_3Cl$]: blue-green tetrahedron; [$PCO_3$]: yellow tetrahedron; Cl: red small ball. (For interpretation of the references to colour in this figure legend, the reader is referred to the web version of this article.)

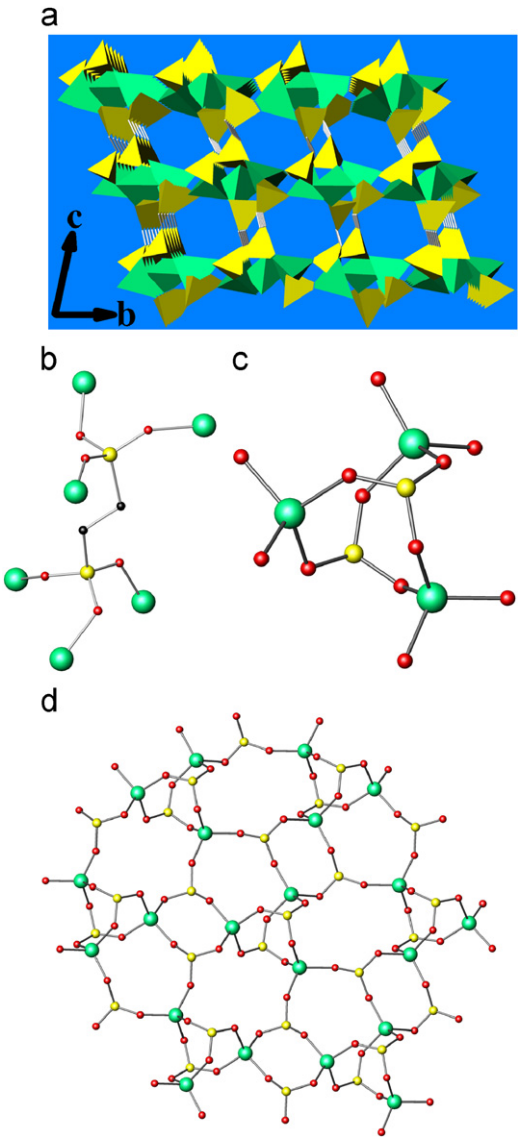


**Fig. 2.** (a) Polyhedral view of the 3D framework, and ball-stick view of (b) the coordination mode for $O_3P(CH_2)_2PO_3$ group, (c) the trinuclear unit and (d) the hybrid layer in **2**. [$ZnO_4$] and [$PCO_3$] are represented by green and yellow tetrahedrons, respectively. (For interpretation of the references to colour in this figure legend, the reader is referred to the web version of this article.)

is same to those in $[(NH_4)(H_3N(CH_2)_2NH_3)_{0.5}Zn_3(O_3P(CH_2)_2PO_3)_2]$ and $[(NH_4)_2Zn_3(O_3P(CH_2)_3PO_3)_2]$ [17]. Thus, two [$PCO_3$] tetrahedral combine three [$ZnO_4$] tetrahedral *via* sharing six corners to form a trinuclear unit, which consists of three 4MRs. Furthermore, each trinuclear unit contact with surrounding six trinuclear units through O–P–O into a single organic–inorganic hybrid layer, which contains 4MRs, 6MRs and 8MRs. Finally, the hybrid layers are pillared by $O_3P(CH_2)_2PO_3$ groups to form 3D open-framework with 1D channel along an *a* axis, which is similar to those of pillared zinc diphosphonates [16,50].

The protonated 1,4-butanediamine is encapsulated into the channel through hydrogen bondings between the protonated nitrogen donors and phosphonate oxygen atoms. The distances of N…O lie in the range 2.77(2)~3.02(2) Å.

### 3.2. Thermal stability

Thermogravimetric analysis (TGA) illustrate that under air atmosphere there is little weight loss up to 250 °C for compound **1**. Upon further heating, an abrupt weight loss stage starts from 320 °C, due to the decomposition of 1,4-butanediamine and $(O_3PCH_2)_2NCH_2PO_3H$ groups. In addition, after as-prepared **1** was annealed at 250 and 300 °C under air atmosphere for 2 h and cooled to room temperature, respectively, both powder XRD patterns are in agreement with those of the as-prepared **1**, which indicates little change of the framework. However, powder XRD

patterns indicate that the 3D framework has collapsed and changed into an amorphous phase after the as-prepared **1** was annealed at 330 °C under air atmosphere for 2 h. This result accords with that of TGA. TGA reveals that under air atmosphere there is an abrupt weight loss stage which starts from 400 °C for the decomposition of 1,4-butanediamine and $O_3P(CH_2)_2PO_3$ groups. Furthermore, after the as-prepared **2** was annealed at 250, 300, 320 and 350 °C under air atmosphere for 2 h and cooled to room temperature; these powder XRD patterns are all in agreement with those of the as-prepared **2**, which indicate little change of the framework.

### 3.3. *Luminescent properties*

Solid-state luminescent properties of solids **1**–**2** were investigated under an ambient temperature. As shown in Fig. 3, solid **1** displays blue emission with a maximum band at 452 nm (excited at 365 nm), while solid **2** exhibits purple emission with a maximum band at 439 nm (excited at 356 nm). Since the excitation profiles of solid **1** are similar to that of solid **2**, and the UV diffuse reflectance spectra of solids **1**–**2** are in accord with that of 1,4-diaminobutane dihydrochloride, as well as 1,4-butanediamine can also emit purple emission with a maximum band at 421 nm (excited at 370 nm), the emission for solids **1**–**2** may probably be assigned to the intraligand fluorescent emission of the protonated 1,4-butanediamine. It is interesting to mention that fluorescent peak bands of solids **1** and **2** exhibit 31 and 18 nm red-shift compared to that of 1,4-butanediamine, respectively. The red-shift may be due to the protonation of 1,4-butanediamine, due to the fluorescent peak band of acidified 1,4-diaminobutane solution also shows 4 nm red-shift compared to that of 1,4-diaminobutane [16]. These results provide an effective method to prepare luminescent solids by the incorporation of luminescent guests into the channel of 3D framework, which can enhance thermal stability and tune peak bands.

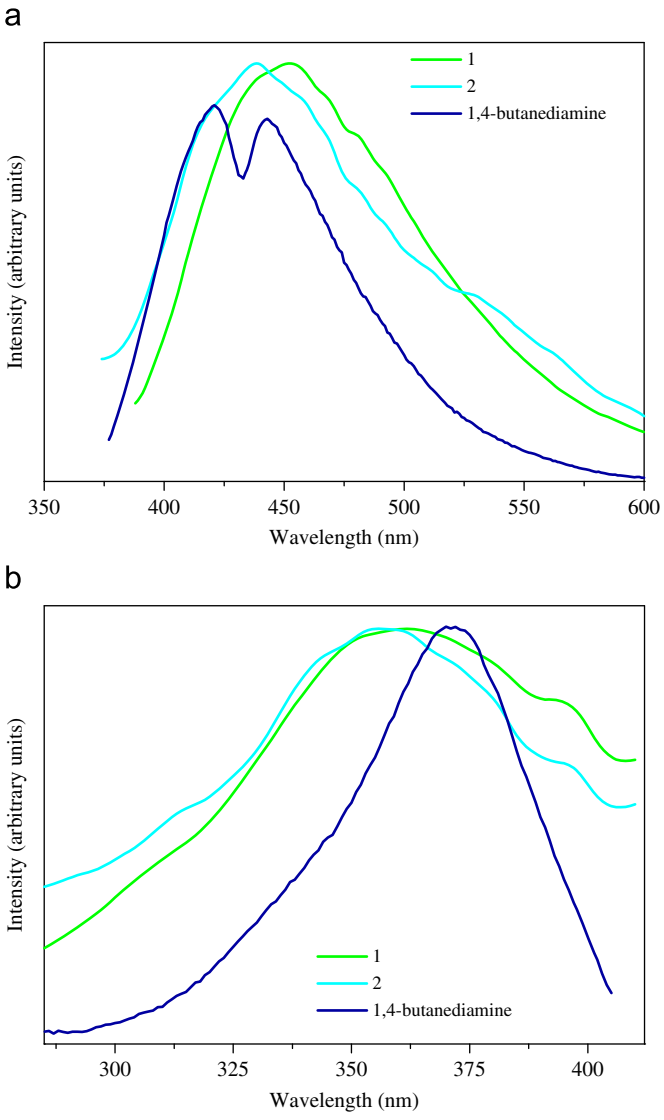


**Fig. 3.** Normalized emission (a) and excitation (b) spectra of solids **1–2**, and 1,4-butanediamine.

## 4. Conclusions

In summary, we have described the syntheses and crystal structures of two new 3D zinc phosphonates, $[(H_3N(CH_2)_4NH_3)Zn_2((O_3PCH_2)_2NCH_2PO_3H)(Cl)]$ (**1**) and $[(H_3N(CH_2)_4NH_3)Zn_3(O_3P(CH_2)_2PO_3)_2]$ (**2**). In **1**, each tetranuclear unit contacts with surrounding six tetranulcear units to form a 3D framework with the 16MR channel. While in **2**, each trinuclear unit interacts with surrounding six trinuclear units through O–P–O into a single hybrid layer, which is further pillared by $O_3P(CH_2)_2PO_3$ groups to form 3D open-framework with 1D channel. In both compounds, 1,4-butanediamines are protonated and encapsulated into the channel through hydrogen bondings. Solids **1** and **2** display blue and purple emissions, respectively. Solids **1** and **2** are thermally stable up to 300 and 350 °C under air atmosphere, respectively. Future efforts are focused on selecting interesting organic amines as structure-directing agents to expand metal phosphonates and investigate the relationship between structures and properties.

## Appendix. Supplementary data

Crystallographic data (CIF), IR, additional structural figure, TGA curves and powder XRD patterns.

## Acknowledgments

This research was supported by grants from the State Key Laboratory of Structure Chemistry, Fujian Institute of Research on the Structure of Matter, Chinese Academy of Sciences (CAS), the National Ministry of Science and Technology of China (2007CB815301), the National Science Foundation of China (20733003 and 20801055), the Science Foundation of CAS and Fujian Province for research funding support (2009HZ0006-1).

## Appendix A. Supplementary materials

Supplementary data associated with this article can be found in the online version at doi:10.1016/j.jssc.2010.11.013.

## References

[1] A. Clearfield, Metal phosphonate chemistry, in: K.D. Karlin (Ed.), Progress in Inorganic Chemistry, vol. 47, Wiley, New York, 1998, pp. 371–511.
[2] J.G. Mao, Coord. Chem. Rev. 251 (2007) 1493.
[3] E. Matczak-Jon, V. Vienova-Adrabińska, Coord. Chem. Rev. 249 (2005) 2458.
[4] R.M.P. Colodrero, A. Cabeza, P. Olivera-Pastor, A. Infantes-Molina, E. Barouda, K.D. Demadis, M.A.G. Aranda, Chem. Eur. J. 15 (2009) 6612.
[5] D.G. Ding, B.L. Wu, Y.T. Fan, H.W. Hou, Cryst. Growth Des. 9 (2009) 508.
[6] T.H. Yang, Y. Liao, L.M. Zheng, R.E. Dinnebier, Y.H. Sua, Jing Mac, Chem. Commun. (2009) 3023.
[7] H.Y. Liu, Z.J. Zhang, W. Shi, B. Zhao, P. Cheng, D.Z. Liao, S.P. Yan, Dalton Trans. (2009) 4416.

[8] L.R. Guo, F. Zhu, Y. Chen, Y.Z. Li, L.M. Zheng, Dalton Trans. (2009) 8548.
[9] D. Cave, F.C. Coomer, E. Molinos, H.H. Klauss, P.T. Wood, Angew. Chem. Int. Ed. 45 (2006) 803.
[10] J.A. Groves, S.R. Miller, S.J. Warrender, C. Mellot-Draznieks, P. Lightfoota, P.A. Wright, Chem. Commun. (2006) 3305.
[11] D.K. Cao, J. Xiao, J.W. Tong, Y.Z. Li, L.M. Zheng, Inorg. Chem. 46 (2007) 428.
[12] J.M. Liang, G.K.H. Shimizu, Inorg. Chem. 46 (2007) 10449.
[13] D.K. Cao, Y.Z. Li, L.M. Zheng, Inorg. Chem. 46 (2007) 7571.
[14] N.G. Armatas, W. Ouellette, K. Whitenack, J. Pelcher, H. Liu, E. Romaine, C.J. O'Connor, J. Zubieta, Inorg. Chem. 48 (2009) 8897.
[15] C. Serre, J.A. Groves, P. Lightfoot, A.M.Z. Slawin, P.A. Wright, N. Stock, T. Bein, M. Haouas, F. Taulelle, G. Férey, Chem. Mater. 18 (2006) 1451.
[16] R.B. Fu, X.H. Huang, S.M. Hu, S.C. Xiang, X.T. Wu, Inorg. Chem. 45 (2006) 5254.
[17] R.B. Fu, S.M. Hu, X.T. Wu, Cryst. Growth Des. 7 (2007) 1134.
[18] V. Baskar, M. Shanmugam, E.C. Sañudo, M. Shanmugam, D. Collison, E.J.L. McInnes, Q. Wei, R.E.P. Winpenny, Chem. Commun. (2007) 37.
[19] S. Konar, N. Bhuvanesh, A. Clearfield, J. Am. Chem. Soc. 128 (2006) 9604.
[20] J. Wu, Y.L. Song, E.P. Zhang, H.W. Hou, Y.T. Fan, Y. Zhu, Chem. Eur. J. 12 (2006) 5823.
[21] Q. Yue, J. Yang, G.H. Li, G.D. Li, J.S. Chen, Inorg. Chem. 45 (2006) 4431.
[22] X.G. Liu, S.S. Bao, Y.Z. Li, L.M. Zheng, Inorg. Chem. 47 (2008) 5525.
[23] Z.X. Chen, Y.M. Zhou, L.H. Weng, D.Y. Zhao, Cryst. Growth Des. 8 (2008) 4045.
[24] X.M. Zhang, J.J. Hou, W.X. Zhang, X.M. Chen, Inorg. Chem. 45 (2006) 8120.
[25] W. Ouellette, M.H. Yu, C.J. O'Connor, J. Zubieta, Inorg. Chem. 45 (2006) 7628.
[26] W. Ouellette, M.H. Yu, C.J. O'Connor, J. Zubieta, Inorg. Chem. 45 (2006) 3224.
[27] R.B. Fu, S.M. Hu, X.T. Wu, Dalton Trans. (2009) 9440.
[28] R.B. Fu, S.M. Hu, X.T. Wu, Inorg. Chem. 46 (2007) 9630.
[29] H.H. Song, P. Yin, L.M. Zheng, J.D. Korp, A.J. Jacobson, S. Gao, X.Q. Xin, Dalton Trans. (2002) 2752.
[30] H.H. Song, L.M. Zheng, Z.M. Wang, C.H. Yan, X.Q. Xin, Inorg. Chem. 40 (2001) 5024.
[31] B. Liu, P. Yin, X.Y. Yi, S. Gao, L.M. Zheng, Inorg. Chem. 45 (2006) 4205.
[32] L.M. Zheng, S. Gao, P. Yin, X.Q. Xin, Inorg. Chem. 43 (2004) 2151.
[33] B. Liu, Y.Z. Li, L.M. Zheng, Inorg. Chem. 44 (2005) 6921.
[34] H.H. Song, L.M. Zheng, C.H. Lin, S.L. Wang, X.Q. Xin, S. Gao, Chem. Mater. 11 (1999) 2382.
[35] L.M. Zheng, H.H. Song, C.H. Lin, S.L. Wang, Z. Hu, Z. Yu, X.Q. Xin, Inorg. Chem. 38 (1999) 4618.
[36] K. Moedritzer, R.R. Irani, J. Inorg. Nucl. Chem. 22 (1961) 297.
[37] A.K. Bhattacharya, G. Thyagarajan, Chem. Rev. 81 (1981) 415.
[38] G.M. Sheldrick, SHELXT 97, Program for Crystal Structure Refinement, University of Göttingen, Germany, 1997.
[39] F. Cecconi, C.A. Ghilardi, P.A.L. Luis, S. Midollini, A. Orlandini, D. Dakternieks, A. Duthie, S. Dominguez, E. Berti, A. Vacca, J. Chem. Soc., Dalton Trans. (2001) 211.
[40] J.G. Mao, Z.K. Wang, A. Clearfield, New J. Chem. 26 (2002) 1010.
[41] H.S. Martinez-Tapia, A. Cabeza, S. Bruque, P. Pertierra, S. Garcia-Granda, M.A.G. Aranda, J. Solid State Chem. 151 (2000) 122.
[42] M. Bishop, S.G. Bott, A.R. Barron, Chem. Mater. 15 (2003) 3074.
[43] L. Cunha-Silva, L. Mafra, D. Ananias, L.D. Carlos, J. Rocha, F.A.A. Paz, Chem. Mater. 19 (2007) 3527.
[44] K.D. Demadis, S.D. Katarachia, M. Koutmos, Inorg. Chem. Commun. 8 (2005) 254.
[45] K.D. Demadis, C. Mantzaridis, P. Lykoudis, Ind. Eng. Chem. Res. 45 (2006) 7795.
[46] K.D. Demadis, S.D. Katarachia, R.G. Raptis, H. zhao, P. Baran, Cryst. Growth Des. 6 (2006) 836.
[47] A. Cabeza, X. Ouyang, C.V.K. Sharma, M.A.G. Aranda, S. Bruque, A. Clearfield, Inorg. Chem. 41 (2002) 2325.
[48] I. Svobodová, P. Lubal, J. Plutnar, J. Havlíčková, J. Kotek, P. Hermann, I. Lukeš, Dalton Trans. (2006) 5184.
[49] V. Chandrasekhar, S. Kingsley, B. Rhatigan, M.K. Lam, A.L. Rheingold, L.M. Zheng, H.H. Song, C.H. Lin, S.L. Wang, Z. Hu, Z. Yu, X.Q. Xin, Inorg. Chem. 41 (2002) 1030.
[50] R.B. Fu, S.M. Hu, H.S. Zhang, L.S. Wang, X.T. Wu, Inorg. Chem. Commun. 8 (2005) 912.